

# Report

---

**To** : MET/MK Marianne König  
**From** : MET/TJH Tim Hewison  
**Copy** :  
**Ref.** : EUM/MET/REP/08/0196, v1B  
**Date** : 26 May 2008

---

**Subject** : **MSG\_Ice\_Contamination**

## 1 BACKGROUND

The inter-calibration of Meteosat with IASI during 2007 [[EUM/MET/REP/08/0052](#)] revealed a bias in the 13.4  $\mu\text{m}$  channel of Meteosat-8 and -9, which became worse during the year. These biases changed abruptly after the decontamination procedures conducted on Meteosat-8 in February 2008 and Meteosat-9 in December 2007. This supports the theory that the bias can be (at least partly) explained by a build-up of (water) ice in the cold optics due to condensation of outgassing material from the spacecraft.

This report considers this theory of contamination and attempts to model its impact on the calibration bias of MSG's infrared (IR) channels. These predictions are then compared with observations – both in the form of inter-calibration of MSG with IASI, and by examination of MSG's relative gain changes before and after decontamination procedures.

## 2 THEORY

The basic hypothesis to be tested here is that the change in bias of the MSG channels is (at least) partly due to a build-up of “ice”, which condenses on the surfaces of the cold optics after outgassing from other material on the satellite. This process has been known about since at least the time of Meteosat First Generation [Schmetz *et al.*, 1994].

This material is most likely to be water ice [Blumstein, 2008]. However, since the rates of outgassing and condensation are unknown, it is not possible to estimate the probable ice thickness on purely theoretic grounds. This can only be inferred from previous experience and from studies such as this. However, it may be assumed that the rate of outgassing decreases exponentially with time since the satellite launch. Furthermore, it is not known exactly where in the instrument optics the ice is likely to condense, although in SEVIRI, the first surfaces to trap contaminants are the optical bandpass filters inside the cold IR optical bench [Pasternak, 2007]. The effect of contamination is difficult to assess because it depends

on the optical characteristics of the optical surfaces that receives contaminants and their coatings' characteristics are not known. The contamination will effect both the gain of the associated channels, as well as their Spectral Response Functions (SRFs). Both these processes could influence the final calibrated radiances produced by the instrument.

## **2.1 Decontamination Procedure**

In-orbit condensation of particle or chemical contamination on the cold optics of the SEVIRI must be periodically removed to ensure that the instrument remains within the acceptable mission limits. The process is relatively simple, however it does take several days. It is anticipated that the operation will be carried out once or twice a year to obviate this degradation. Heaters are employed to warm the detector optics causing the contaminants to evaporate after which the instrument is allowed to cool down back to 95 K.

Meteosat-8 and -9 were launched on 28 August 2002 and 21 December 2005, respectively. Spacecraft decontaminations were performed on Meteosat-9 between 11 – 15 December 2006 and 3 - 10 December 2007, and on Meteosat-8 between 26 – 29 June and 11 – 18 December 2006 and in January 2008.

## **2.2 Ice Transmission Models**

CNES provided results of an ice transmission model used on IASI [Blumstein, 2008]. This model has compared very well with the IASI measurements for a range of ice thicknesses from 12 nm to 3.7  $\mu\text{m}$ , except for the short wave range – above 2000  $\text{cm}^{-1}$ . The model is not applicable at wavelengths less than 5  $\mu\text{m}$  because thin film effects are superposed to the main absorption effect. These effects depend on the optical coating that is under the ice film and cannot be extrapolated from the IASI in-flight data [Blumstein, 2008].

Additional ice transmission model data was also obtained from Astrium [Pasternak, 2007]. This model assumes the optics are coated in a material that provides a transmission of 90% in addition to a layer of ice. The transmission is estimated for different ice thicknesses, from 125 nm to 2  $\mu\text{m}$ , providing a range of contamination losses compatible to those observed.

The Astrium data stops short of the long-wave end of the 13.9  $\mu\text{m}$  channel and has to be extrapolated, which leads to large uncertainties in this channel. However, as will be shown, the CNES data presented here<sup>1</sup> does not extend to sufficiently thick ice. So, although neither dataset provides definitive results, it is hoped that together they can provide a good approximation to realistic absorption spectra of ice over appropriate range of thicknesses.

The ice transmission models are plotted together in Figure 3, which also shows the SRFs of the SEVIRI infrared channels on Meteosat-8. Figure 4 shows the modelled transmission as a function of ice thickness for a single channel at the centre of the 12  $\mu\text{m}$  ice absorption band. The two models give somewhat different results for comparable ice thickness.

---

<sup>1</sup> In fact, the CNES data is applicable to ice thicknesses up to 3.7  $\mu\text{m}$ , so the analysis could be extended.

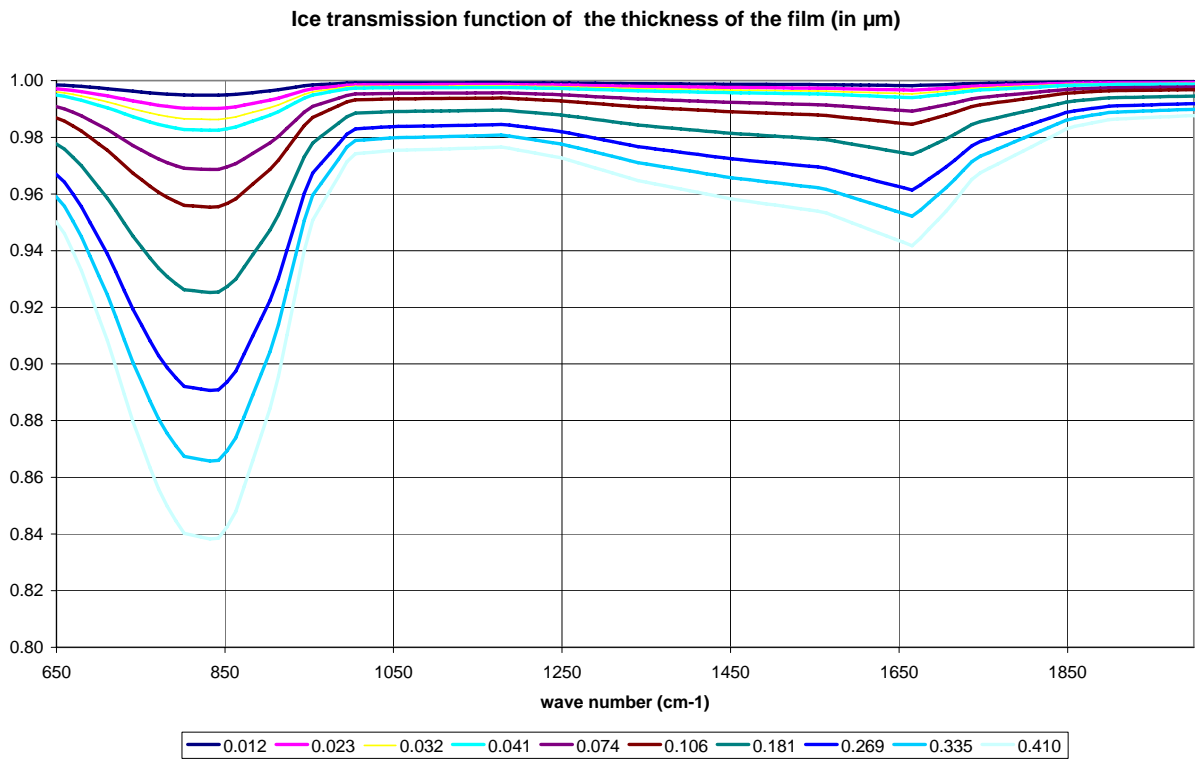


**Figure 1 Ice transmission model data from CNES for ice layers 0.012 – 0.410  $\mu\text{m}$  thick.**

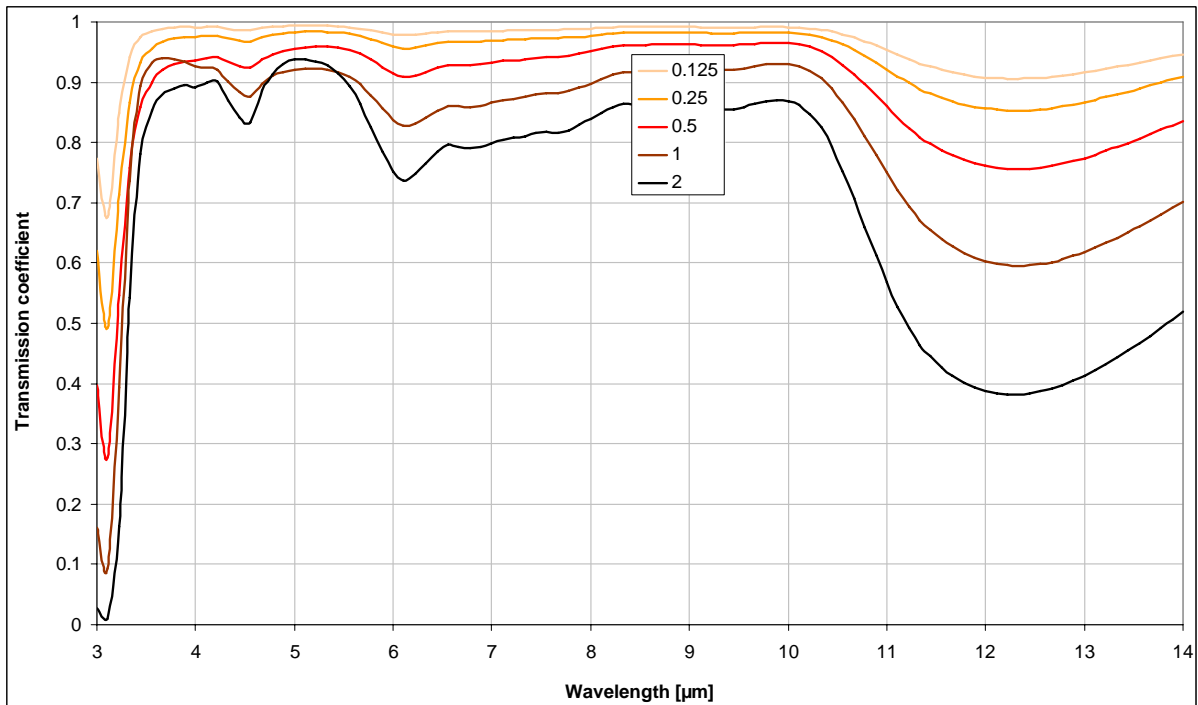


**Figure 2 Astrium ice transmission model for ice layer of 5 thicknesses: 0.125 – 2  $\mu\text{m}$ .**

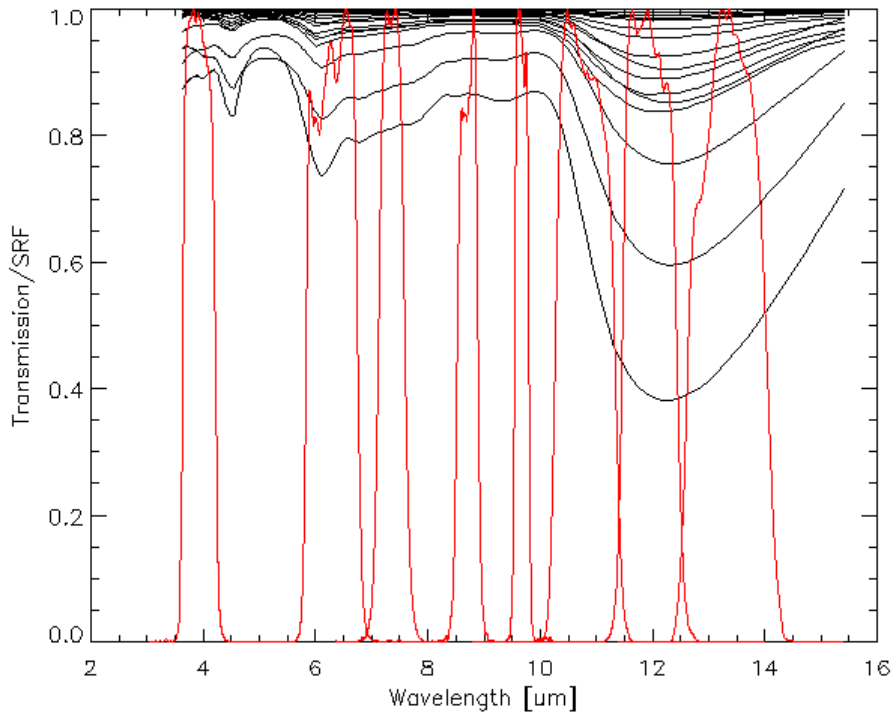


**Figure 3** Transmission spectra of ice layers of different thicknesses (black): 12, 23, 32, 41, 74, 106, 125, 181, 250, 269, 335, 410, 500, 1000 and 2000 nm layers. Spectral Response Functions of Meteosat-8 infrared channels (red).

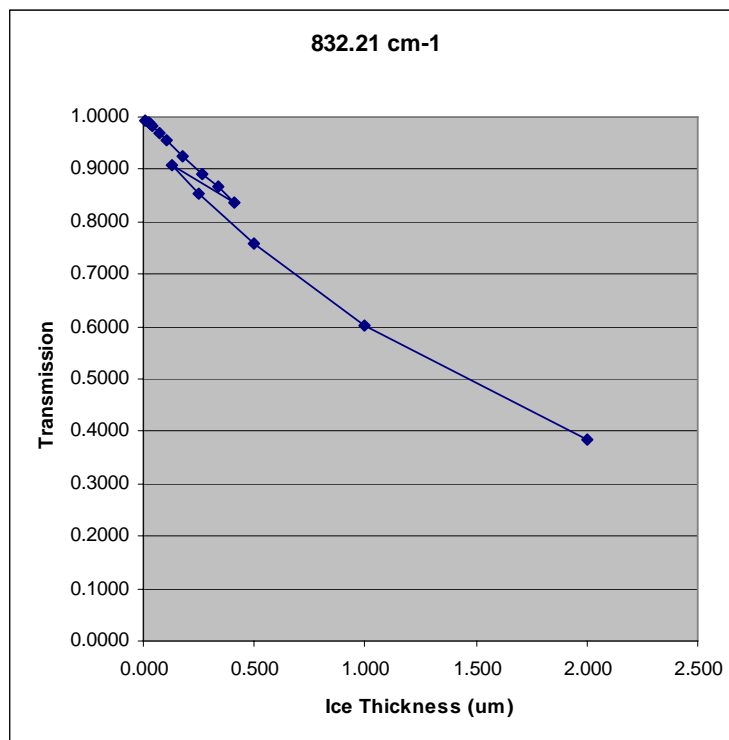


**Figure 4** Comparison of 2 models' predicted transmission for ice of different thickness at the centre of ice's 12  $\mu\text{m}$  absorption band. Each point represents transmission through ice layer of different thickness, corresponding to CNES model in Figure 1 (smaller range, higher transmission) and Astrium model in Figure 2 (larger range, lower transmission).

### 2.3 Modification of Spectral Response Functions

Differential absorption by this ice layer would modify the instrument's spectral response function (SRF). Although much of this would be accounted for in the internal calibration processes, any unidentified changes in the SRF could bias the observed scene radiances. It is possible to investigate whether this is a feasible explanation of the bias in the 13.4  $\mu\text{m}$  channel, or whether other proposed shifts in the SRFs are feasible, by repeating the inter-calibration process after applying these changes to the SRFs.

The radiance,  $L$ , measured by an unmodified instrument, with spectral response function,  $r_v$ , viewing a scene with radiance spectrum,  $L_v$ , is:

$$L = \frac{\int L_v r_v d\nu}{\int r_v d\nu} \quad (1)$$

When viewing a hot black body calibration target, with radiance  $B_v(T_H)$ , the unmodified instrument sees a radiance,  $L_H$ :

$$L_H = \frac{\int B_v(T_H) r_v d\nu}{\int r_v d\nu} \quad (2)$$

Viewing this scene when the SRF is convolved with a transmittance,  $\tau_v$ , the radiance,  $L_H'$ , is:

$$L_H' = \frac{\int B_v(T_H) r_v \tau_v d\nu}{\int r_v \tau_v d\nu} \quad (3)$$

Assuming the space view radiances remain as zero, the apparent gain of the instrument,  $G'$  is:

$$G' = \frac{L_H'}{L_H} \quad (4)$$

This gain is then applied to calculate the apparent radiance of a scene,  $L'$ , viewed by an instrument with SRF,  $r_v$ , modified by a layer of ice with transmission,  $\tau_v$ :

$$L' = \frac{\int L_v r_v \tau_v d\nu}{\int r_v \tau_v d\nu} \frac{L_H'}{L_H} \quad (5)$$

To evaluate the difference between  $L'$  and  $L$ , a typical scene radiance spectrum,  $L_v$ , was taken from a single IASI observation (on 07/07/07 21:00 0N at 0°N, 0°S).  $L' - L$  was evaluated over a range of transmission spectra,  $\tau_v$ , given in Figure 4. The results are expressed in terms of brightness temperatures in Figure 5.

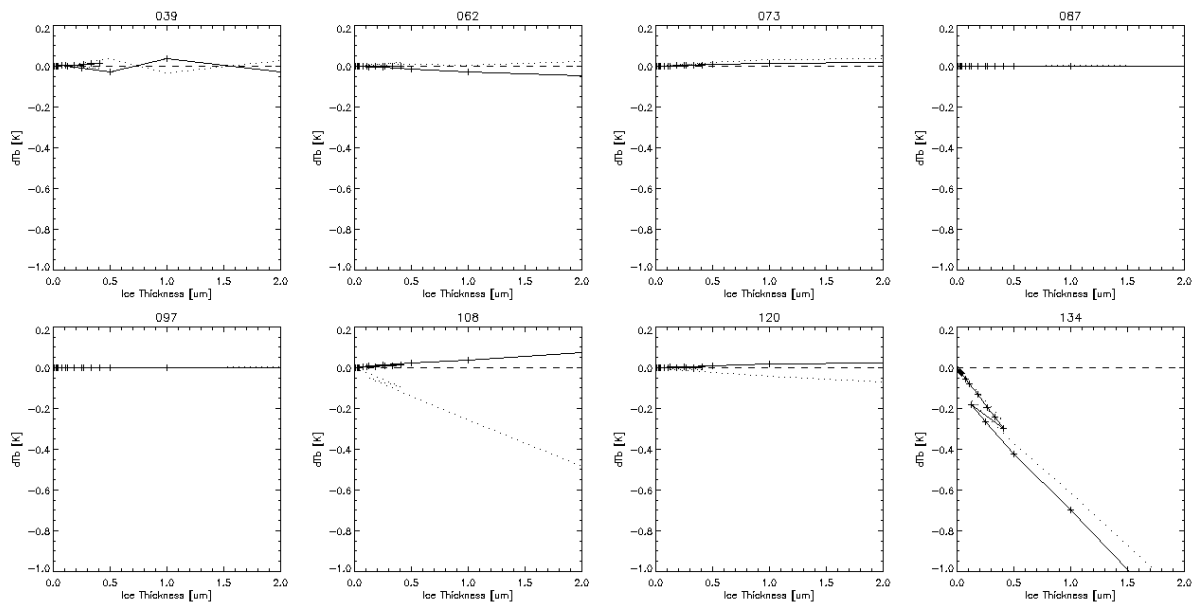


**Figure 5** Bias in brightness temperatures modelled by modifying Meteosat-8's SRF by the absorption of different thicknesses of ice, following the 2 models described above. Solid line with crosses shows the predicted differences in brightness temperature compared with the uncontaminated instrument, accounting for calibration gain changes. The dotted line shows the result without accounting for these gain changes.

The 13.4  $\mu\text{m}$  channel, which is on the edge of the ice absorption band, is predicted to be most sensitive to ice contamination. This is because the ice is modifying the SRF of this channel, which lies on the edge of an atmospheric  $\text{CO}_2$  absorption band. The resulting  $\sim 0.7$  K change in bias of the 13.4  $\mu\text{m}$  channel bias for an ice thickness of 1  $\mu\text{m}$  is consistent with the observed changes during the course of 2007. The bias in the other channels is predicted to be negligible over this range of ice thickness.

If the gain modification term is neglected from the expression for  $L'$  in Eqn (5), the resulting differences are shown by the dotted lines in Figure 5. In this case, the channels close to the edge of the 12  $\mu\text{m}$  ice absorption feature are most affected by the contamination (10.8 and 13.4  $\mu\text{m}$ ). This shows the gain changes are particularly important in the 10.8  $\mu\text{m}$  channel, which otherwise would also show a strong sensitivity to ice contamination. Because this is a window channel, it typically samples scenes with radiance spectra similar to that of a black body, which are not strongly affected by the change in SRF.

Meteosat-8 and -9 have slightly different SRFs, but yield very similar results – so only the former results are shown here. These calculations are for 'a typical' clear sky scene, calculated from 'a typical' IASI radiance spectrum. It will, of course, be different for scenes with different radiances – typically, larger errors for scenes further from the brightness temperature of the black body calibration target. The results should be processed through the whole EUMETSAT Image Processing Facility (IMPF) to check their validity as this method is a simplification of the calibration process.

## 2.4 Modification of the Radiometer Equation

The above analysis does not explicitly account for thermal emission from an ice layer on the optics when viewing the cold space calibration view. This would increase the space view radiance slightly. This would cause the gain to be underestimated when comparing the calibration views of space and the ambient black body target. However, such an effect would be removed by the calibration process, resulting in zero net change in the scene radiances. As the ice is at a very low temperature ( $\sim 95$  K), its thermal emission is also very low, so this effect is very small ( $<5\%$ ) compared to that of the change to the SRFs.

## 3 OBSERVATIONAL EVIDENCE

### 3.1 Meteosat-IASI inter-calibration

Figure 6 and Figure 7 show the time-series of the relative bias for Meteosat-8 and -9, respectively, over the period 1 Jan 2007 to 30 April 2008. Most channels show small differences ( $<1$  K), although the  $13.4 \mu\text{m}$  channel of Meteosat-9 shows a large bias. These time series also show the biases in this channel changed during 2007, followed by a sudden recovery following the decontamination procedure of 3-11 December. The biases in the other channels remain almost constant, with small standard deviations  $\sim 0.05$  K.

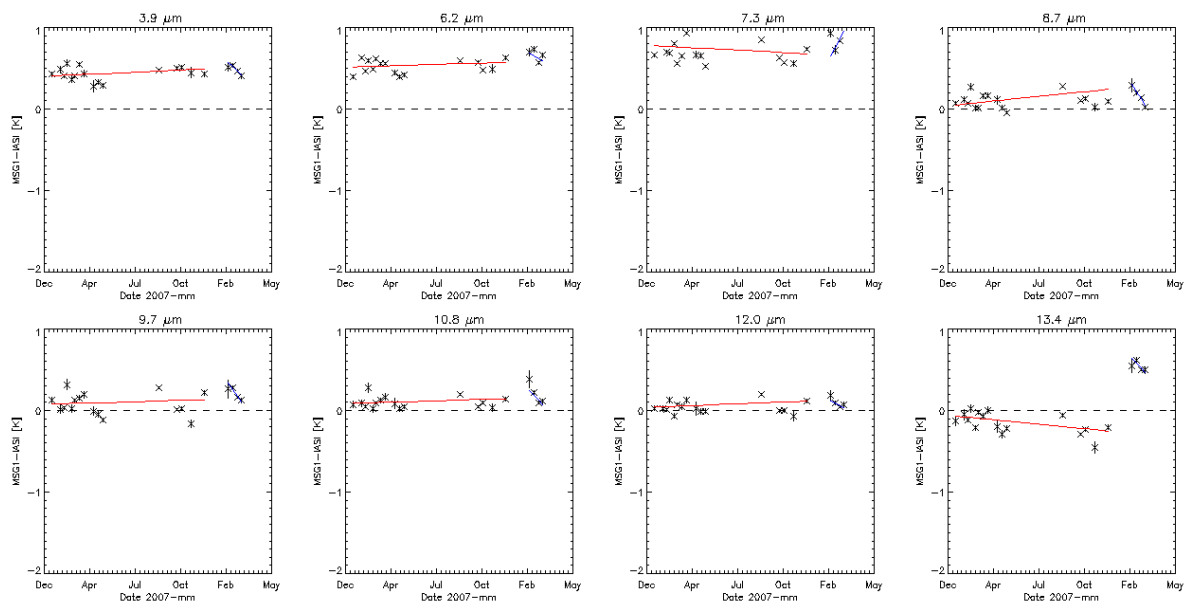


**Figure 6** Time series of relative bias (Meteosat-8 – IASI) from all successful inter-comparisons over period Jan 2007 to April 2008. Points show mean bias for reference scene radiance with  $1-\sigma$  uncertainty shown by error bars. Solid lines show linear regressions fitted to data before (red) and after (blue) decontamination procedure.

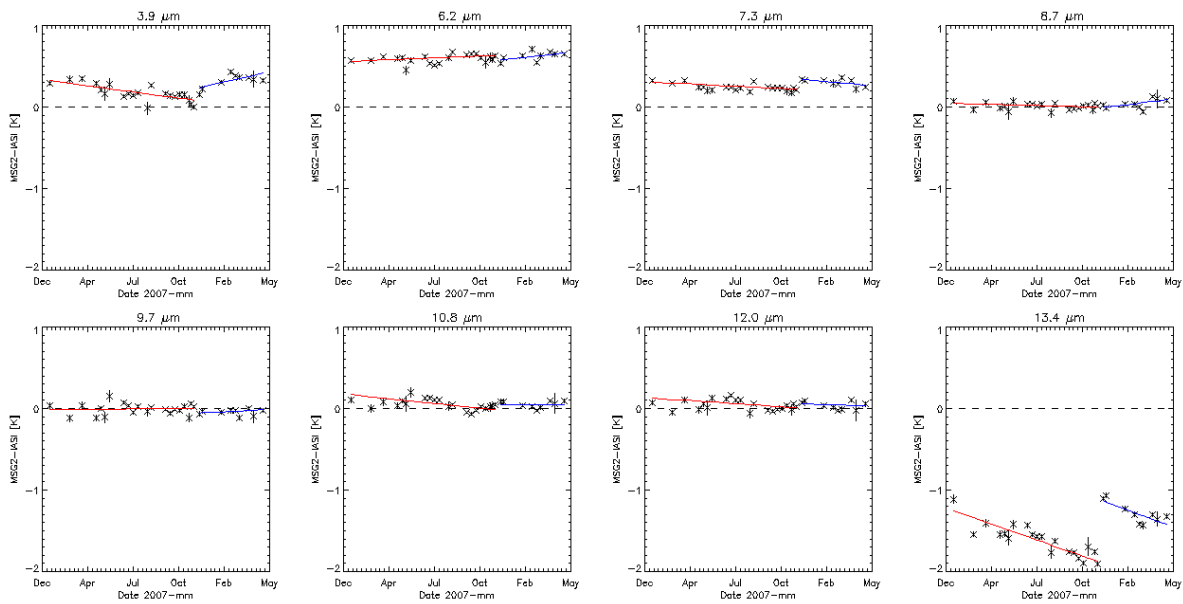


Figure 7 As Figure 6, but for Meteosat-9 – IASI

The trend in the relative bias was calculated using only the 2007 Meteosat-9 data prior to the decontamination procedure in December [Hewison, 2008]. The results showed there were statistically significant trends in the 3.9 and 13.4  $\mu\text{m}$  channels:  $-0.30 \text{ K/yr}$  and  $-0.72 \text{ K/yr}$ , respectively. Cases since January 2008, after the decontamination procedure, confirm the bias in both these channels return to values comparable to those found near the start of 2007.

The observed trend during 2007 in the 3.9  $\mu\text{m}$  channel Meteosat-9 was not expected from the model results shown in Figure 5. However, since the decontamination, the relative bias in this channel has returned to levels similar to those experienced at the same time in 2007. This suggests the bias may have a contribution from an annual cycle of scene radiances.

We can assume the instrument is free of ice immediately after a decontamination procedure. However, ice will begin to condense quickly, so we do not have exact measurements. This was then followed by further degradation.

Meteosat-9 is younger than Meteosat-8 – hence it outgases more rapidly and the bias deteriorates more quickly. However, the 13.4  $\mu\text{m}$  channels of both Meteosat-8 and -9 both showed jumps of  $\sim +0.8 \text{ K}$  during the decontamination procedures of February 2008 and December 2007, respectively. It is surprising that both instruments increase by similar amounts, given the slower rate of deterioration found for Meteosat-8 and the fact that it was little over 1 year since its last decontamination.

### 3.2 Meteosat Gain Changes on Decontamination

We find a change in gain in the 12.0  $\mu\text{m}$  channel following the decontamination consistent with a 50% transmission loss [Table 6 of Müller, 2008]. From Figure 4 we see this is consistent with transmission through an ice layer  $\sim 1 \mu\text{m}$  thick, similar to that required to produce a change in bias of  $\sim 0.7 \text{ K}$  for typical scene radiances, as shown in Figure 5.

## **4 CONCLUSIONS**

The observed changes in bias are consistent with the model predictions of Figure 5 for an ice layer increasing in thickness from 0 to  $\sim 1 \mu\text{m}$  during the period between decontaminations. This causes the bias in the  $13.4 \mu\text{m}$  channel to change by  $\sim 0.7 \text{ K/yr}$ , due to changes in its SRF, but has no net effect on the other channels, as it is removed by the calibration.

## **5 RECOMMENDATIONS**

The surprising result that the  $13.4 \mu\text{m}$  channels of both Meteosat-8 and -9 jumped by similar magnitudes after their respective recent decontaminations should be checked in future decontamination procedures.

Based on these results, it is important to continue routine inter-calibration of Meteosat with IASI. Operational corrections could be derived for the biases caused by ice contamination. However, this theory should be further tested by processing data through the whole EUMETSAT Image Processing Facility (IMPF) to check their validity as this method is a simplification of the calibration process.

## **6 REFERENCES**

Denis Blumstein, personal communication, 12 March 2008

Hewison, T. J., 2008: The inter-calibration of Meteosat with IASI during 2007 [[EUM/MET/REP/08/0052](#)]

Müller, J., 2008: MSG IR 13.4 Calibration Stability [EUM/OPS-MSG/TEN/06/0206]

Fred Pasternak (Astrium), personal communication 05 June 2007.

Johannes Schmetz, Leo van de Berg and Volker Gärtner, 1994: *Calibration of the Meteosat IR and WV Channels for Cloud Studies and Wind Extraction*, Proceedings of 10<sup>th</sup> Meteosat Scientific Users' Conference, Cascais, Portugal, 5-9 September 1994.